MICHIGAN STATE UNIVERSITY

CYCLOTRON LABORATORY

EXPERIMENTAL OBSERVABLES AND THE NUCLEAR EQUATION OF STATE

LÀSZLÒ P. CSERNAI

OCTOBER 1987

MSUCL-623

MSUCL - 623
October, 1987

Experimental Observables and The Nuclear Equation of State[†]

Làszlò P. Csernai[*]

National Superconducting Cyclotron Laboratory
Michigan State University
East Lansing, Michigan 48824-1321, USA

September 1987

[†]Invited Seminar Lecture at the International School of Physics "Enrico Fermi", Varenna, Italy, June 23 - July 3, 1987.

Experimental Observables and The Nuclear Equation of State[†]

Làszlò P. Csernai[*]
National Superconducting Cyclotron Laboratory
Michigan State University

In this lecture I would like to mention two observables which might help us to shed light on the problems related to the equation of state (EOS) of nuclear matter. In particular, their relations to the nuclear liquid - gas phase transition, which is expected to occur below normal nuclear densities at temperatures below T≈15 MeV. The observables are not new: the collective transverse flow, and the abundances of composite fragments. These measurables together with others: like the slope of the fragment energy spectra, population ratios of different excited levels of the fragments, small and large angle p, π, d interferometry, π-multiplicities, etc. have been used already in attempts to extract information on the nuclear EOS. Since the most important basic facts have been mentioned already in Professor Greiner's lecture at this school I will confine my talk to the above mentioned two observables.

Theoretically the existence of the nuclear liquid-gas phase transition follows from the basic features of the nucleon-nucleon interaction. Namely from the short range repulsion and a longer range attraction. This type of interaction leads to a Van der Waals type of behaviour in most theoretical models. Also the saturation properties of normal nuclear matter are the consequence of this interaction.

The basic problem is, that even if the phase transition exists, can we observe its consequences in a nuclear collision, because this is a rather small system and also short lived. Today this is still an open question. However, there are some hints in the present observables which may be related to the phase transition. One such hint is the recently observed deviation in the scaling behaviour of the collective transverse flow [1]. The other hint arises from an effect, which was pointed out earlier [2],

namely that the entropy extracted from light and heavy fragment abundances shows a difference. There are experiments pointing towards this direction [3-4], however, neither the theoretical analysis can be considered as final nor the experimental data are complete in this area yet.

The lecture will be divided into two parts. In the first part we will discuss the transverse flow analysis and the scaling properties of the collective flow occuring in nuclear collisions. Then we will apply this scaling analysis to the transverse flow measurements. In the second part, we will briefly review the static statistical fragmentation models, their successes and failures in explaining experimental data and we will discuss the possibilities to improve these static fragmentation models. Dynamic fragmentation models are discussed in other lectures at this school (Greiner, Gregoire, Ngo).

I. COLLECTIVE TRANSVERSE FLOW

The fluid dynamics is a macroscopic theory, which refers directly to thermodynamical concepts. The equation of state serves as an input of the Euler or Navier-Stokes equations. In this model, compression effects give rise to a flux of particles in the direction perpendicular to the beam (side-splash) for central collisions (b=0), and to a bounce-off of projectile-like fragments away from the high-density region at intermediate impact parameters [5-7].

Ideally, exclusive measurements in 4π-detectors should give information about the collective flow processes. If A, Z, and $\vec{p}$ are known for all the emitted fragments, the reaction plane can be estimated [8-9] and an analysis in terms of global variables (e.g. the sphericity tensor) is possible. This allows the determination of quantities such as the mean flow angle, θ, and the shape of the momentum distribution. Several types of detectors are available today, which come close to an acceptance of 4π sr. Electronic-type detectors, ranging from the Plastic Ball/Plastic Wall spectrometer to time-projection chambers have been developed and used in heavy-ion measurements. Visual-type detectors such as streamer chambers and nuclear

emulsions have been borrowed from high-energy physics and rather successfully employed in nuclear experiments. A new technical development is the use of charge-coupled device (CCD) cameras with a streamer chamber. The introduction of solid-state image sensors in place of photographic film promises to alleviate the most problematic features in streamer chamber measurements.

An Overview of The Collective Flow Analysis

When all charged particles are measured in an event one can and should introduce global observables. One of these is the sphericity tensor. The sphericity tensor is defined as:

$$S_{ij} = \sum_{\nu} \omega_{\nu} p_i(\nu)\, p_j(\nu)$$

where p_i and p_j are two components of the momentum $\vec{p} = (p_x, p_y, p_z)$ of a particle ν in a given event, and ω_ν is a weight factor associated with each particle. If the weight factor is $\omega_\nu = 1$ for all particles we speak about the sphericity tensor, if $\omega_\nu = 1/(2m_i)$ then S_{ij} (or F_{ij}) is the energy flow tensor. If this tensor is diagonalized, the three eigenvalues have the magnitudes: f_1, f_2, and f_3, and the orientation of the tensor is characterized by the 3 eigenvectors.

With this procedure, the distribution of the momenta within an event is represented by an ellipsoid of semi-axes f_1, f_2, and f_3. Thus, the shape of the momentum distribution can be evaluated and compared with the predictions of different theoretical models. A particularly interesting parameter is θ the flow angle. This is the polar angle between the beam axis and the eigenvector corresponding to the largest eigenvalue.

In determining this quantity experimentally, large distortions due to finite-multiplicity effects are introduced. Danielewicz and Gyulassy have shown that these distortions arise from the jacobian of the transformation which relates the flow parameters f_1/f_3 and θ to the six independent matrix elements [10]. They concluded that an unambiguous sign of the collective

sidewards flow can be obtained if the distribution of the flow angles in a sample of many events:

$$\frac{dN(\theta)}{d(\cos\theta)}$$

peaks at a finite angle (here N is the number of events which yield a flow angle of θ, after diagonalizing the energy flow tensor F_{ij}).

Several experiments have been performed to study the flow angle distributions for various systems at different energies using the Plastic Ball spectrometer [9-11]. The experimental distributions clearly show a sideward flow, especially for heavier systems. Theoretical models reproduce the collective transverse flow effect only if the repulsive nucleon nucleon interactions are taken into account. This can be done in the fluid dynamical model by using an Equation of State, or in the transport theoretical models (BUU-VUU) [12-13] with the inclusion of a density (and recently also momentum) dependent main field. The transverse flow indicates a rather stiff nuclear matter behaviour especially if the momentum dependence of the main field potential is neglected. The incompressibility K of the nuclear matter is estimated to be of the order of K = 200-350 MeV.

The results reviewed above show that the direction of flow and the beam axis define the reaction plane. If the determination of this plane is possible experimentally, then one can study the distribution of the projected momenta, rather than simply the flow angle.

The main problem with the sphericity analysis is its sensitivity to statistical fluctuations. Danielewicz and Odyniec have suggested a different approach which helps eliminate finite-multiplicity distortions arising from the experimental determination of the reaction plane, and which has been proven to be a more sensitive and powerful tool in revealing collective-flow effects [8]. In brief, the method consists of estimating the reaction plane from the transverse momenta of the emitted particles, and then rotating each event to its reaction plane. The distribution of the average transverse momenta of the emitted particles as a function of rapidity is then studied for evidence of collective effects., Danielewicz and Odyniec have applied

their analysis to the data obtained in an experiment performed at the LBL streamer chamber for the Ar+KCl reaction at 1.8 GeV/nucleon. The same experiment had been previously analysed with the sphericity tensor method, and no conclusive evidence of collective flow was seen[14]. With the transverse momentum analysis, a substantial transverse momentum transfer was found.

The same system was studied by another group [15], again at the LBL streamer chamber. A comparison of their experimental transverse momentum distribution with the predictions of VUU calculations seemed to point towards a "medium" to "stiff" equation of state, with compressibility values ranging between 200 and 300 MeV.

Doss et al. have studied the dependence of collective flow on beam energy, multiplicity, and mass of the system in a series of measurements performed at the Bevalac with the Plastic Ball detector [11]. Ca+Ca, Nb+Nb, and Au+Au collisions were studied at energies between 150 and 1000 MeV/nucleon. To minimize the effects of the detector bias on the quantitative measure of flow, they calculate the slope of the transverse momentum distribution at mid-rapidity, which they call "flow". As predicted by hydrodynamic calculations, and observed in previous experiments [16], the flow increases with the mass of the system. The powerful method of transverse flow analysis made it possible to analyse a series of emulsion measurements with Au and Xe beams, at energies from 0.5 to 1.2 GeV/nucleon [17]. The energy of the projectile is determined from its range in the emulsion, the charge of emitted $Z \geq 2$ particles is obtained from ionization measurements, and A is assumed to be = 2Z. The only other measured quantities are the azimuthal angle ϕ and the polar angle θ of the fragments. Therefore, a quantity called pseudo-transverse momentum, defined as

$$P_\mu^t = \tan \theta_\mu \, P$$

is introduced. Here, P is the longitudinal momentum per nucleon of the beam. The distribution of mean pseudo-P^t per nucleon projected onto the reaction plane, P^x/A, vs. P^t shows a significant collective flow, and the

values extracted are consistent with those obtained in other experiments. A subsequent study based on a simulation by the FREESCO code [18] showed that the result is not surprising and that the success of the method can largely be attributed to the selection of heavier fragments in the latter experiment. As it was shown in theoretical calculations [19-20] the heavy emitted fragments are less subject to thermal fluctuations, and so, they maintain the information on the collective sidewards flow better.

Transverse-Momentum Analysis

The transverse-momentum analysis recently introduced by Danielewicz and Odyniec [8] is now recognized as the most sensitive method to identify collective flow effects in experimental data.

These effects are of particular interest because, in theoretical calculations, they are associated with the compression of nuclear matter during a collision. While the intra-nuclear cascade model, which lacks compression energy, does not predict such collective flow, the hydrodynamical model and the VUU (or BUU) theory, on the other hand, predict a sidewards flow. This varies in magnitude with the beam energy and the mass of the system.

This method involves the detrmination of the reaction plane for each event, by defining a vector $\vec{Q}$ constructed from the transverse momenta of the particles observed in that event, $\vec{p}_\nu$:

$$\vec{Q} = \sum_{\nu=1}^{M} \omega_\nu \vec{p}_\nu \qquad (1)$$

where ν is an index which runs over all the fragments in the event, and ω_ν is a weight factor defined as follows:

$$\omega_\nu \begin{cases} = +1 \text{ for baryons with rapidity } y_\nu > y_{cm}+\delta \\ = -1 \text{ for baryons with rapidity } y_\nu < y_{cm}-\delta \\ = 0 \text{ otherwise} \end{cases} \qquad (2)$$

By setting $\delta \neq 0$, particles around mid-rapidity, which contribute most of the unwanted statistical fluctuations, are removed from the evaluation of the reaction plane. δ should be selected to minimize the fluctuation of the estimated reaction plane. To do this the reaction plane is separately evaluated for each of the two sub-events each containing half the observed particles. Thus, two vectors, $\vec{Q}_I$ and $\vec{Q}_{II}$, are constructed. The azimuthal angle ϕ between $\vec{Q}_I$ and $\vec{Q}_{II}$ is calculated and its distribution for the given sample can be plotted. If a reaction plane really exists, this distribution will peak at $\phi=0$. The value of δ is chosen to minimize the width of the azimuthal angle distribution.

The goal of the calculation is to obtain the transverse momentum per nucleon projected onto the reaction plane. In order to eliminate another type of finite-multiplicity distortion in this estimate, the so called self-correlation term is removed from the calculation of $\vec{Q}$ [8]. An 'estimated' reaction plane is thereby obtained for each particle ν in the event:

$$\vec{Q}'_\nu = \sum_{\mu \neq \nu} \omega_\mu \vec{p}_\mu \qquad (3)$$

The projected transverse momentum per nucleon of the fragment ν, evaluated with respect to this 'estimated' reaction plane, is therefore:

$$p_\nu^{x'} = \vec{p}_\nu \frac{\vec{Q}'_\nu}{|\vec{Q}'_\nu|} \qquad (4)$$

When this quantity has been calculated for all the fragments in all events, its mean value , $\langle p^{x'} \rangle$, is evaluated for each rapidity bin. The obtained $\langle p^{x'}(y) \rangle$ is smaller than the 'true' average transverse momentum (projected onto $\vec{Q}$ rather than $\vec{Q}'_\nu$) by a factor of $\langle \cos \phi \rangle$, where ϕ is the azimuthal angle between $\vec{Q}$ and $\vec{Q}'_\nu$, and

$$\langle p^x(y) \rangle = \langle p^{x'}(y) \rangle / \langle \cos \phi \rangle \qquad (5)$$

The value of $\langle \cos \phi \rangle$, can be estimated by the width of the distribution of the azimuthal angle difference of Q_I and Q_{II} mentioned above.

Scaling Behaviour of Transverse Flow

The basic equations for a perfect nonrelativistic fluid-dynamical description of a nuclear collision are the continuity equation:

$$\frac{\partial \rho}{\partial t} + \vec{\nabla}(\rho \vec{u}) = 0 \ , \tag{6}$$

which relates the mass distribution ρ and the velocity distribution $\vec{u}$; the Euler equation:

$$\frac{\partial \vec{u}}{\partial t} + (\vec{u}\ \vec{\nabla})\vec{u} = -\frac{1}{\rho} P \quad , \tag{7}$$

and the equation of state (EOS), which relates, the pressure P to the density ρ, and the entropy density, s=S/V, of the system:

$$P = P(\rho, s) \tag{8}$$

For a non-viscous fluid the entropy is constant during the expansion, therefore

$$\vec{\nabla} P \approx (\frac{\partial P}{\partial \rho})_s \vec{\nabla}\rho = c_s^2\ \vec{\nabla}\rho \quad , \tag{9}$$

where c_s is the sound velocity.

The above equations with the initial conditions on $\vec{u}$, ρ, and s, determine the hydrodynamical evolution of the system. In Ref. [21] dimensionless, scale-invariant quantities were derived, which can be used to describe the general properties of a system, and also to compare the hydrodynamical behaviour of systems of different masses and energies.

A characteristic mass, m_1, temperature T_1, length l_1, and velocity u_1 can be introduced in a heavy ion collision as:

$$m_1 = mA \tag{10}$$

where m is the nucleon mass and A is the number of nucleons in the system;

$$u_1 = |\vec{u}_0| = \left(\frac{2E_0}{m}\right)^{1/2} \tag{11}$$

where E_0 is the initial c.m. energy per nucleon of the projectile; and

$$l_1^3 = \frac{4}{3}\pi r_0^3 A \tag{12}$$

which represents the volume of the system.

After introducing the definitions $\mathbf{r}=l_1\tilde{\mathbf{r}}$ for the radius, $t=t_1\tilde{t}$ for the time, and $T=T_1\tilde{T}$ for the temperature (where $T_1=2/3\ E_0$), the above characteristic quantities can be utilized to define dimensionless quantities, denoted by a tilde:

$$\rho(r,t) = \frac{m_1}{l_1^3}\tilde{\rho}(\tilde{r},\tilde{t}) \quad , \tag{13}$$

$$u(r,t) = u_1\,\tilde{u}(\tilde{r},\tilde{t}) \ . \tag{14}$$

These characteristic dimensionless hydrodynamical functions are independent of the total mass A and the energy E_0 of the system.

Now, since the sound velocity is of the same order as the thermal velocity of the nucleons, $c= u_1\tilde{c}$, with $\tilde{c}\approx 1$, the continuity and Euler's equations can be rewritten in dimensionless form:

$$m_1\left[\frac{\partial\tilde{\rho}}{\partial\tilde{t}} + S\tilde{\nabla}(\tilde{\rho}\,\tilde{u})\right] = 0 \quad , \tag{15}$$

$$\frac{\partial\tilde{u}}{\partial\tilde{t}} + S(\tilde{u}\,\tilde{\nabla})\tilde{u} = -S\tilde{c}^2\frac{\tilde{\nabla}\tilde{\rho}}{\tilde{\rho}} \quad , \tag{16}$$

where $S=u_1 t_1/l_1$ is the Strouhal number.

In a small system, such as the one formed in a nuclear collision, the role of viscosity should not be neglected. Assuming that the coefficient of bulk viscosity ξ is proportional to the shear viscosity η, ($\xi=q\eta$, where q is a dimensionless constant) and that the kinematic viscosity $\nu=\eta/\rho$ is constant during the expansion, the Navier-Stokes equation can be written (again in dimensionless form) as:

$$\frac{\partial \tilde{u}}{\partial \tilde{t}} + S(\tilde{u}\,\tilde{\nabla})\tilde{u} = -S\tilde{c}^2 \frac{\tilde{\nabla}\tilde{\rho}}{\tilde{\rho}} - \frac{S}{Re}\left[\tilde{\Delta}\tilde{u} + (q+1/3)\tilde{\nabla}\,(\tilde{\nabla}\,\tilde{u})\right], \qquad (17)$$

where Re is the Reynolds number: $Re=l_1 u_1/\nu$. With a proper choice of the time scale, $t_1=l_1/u_1$, S can be set equal to 1. Then the solutions of the hydrodynamical equations depend on $\tilde{r}$, $\tilde{t}$, and the Reynolds number Re only. In this way, the flow patterns of systems of different energies and of different masses are similar if the Reynolds number, $\tilde{r}$ and $\tilde{t}$ are the same.

According to this picture, scale-invariant quantities can be defined, and a deviation from the scale invariance indicates the onset of physical processes which lead to a non-scale-invariant flow in the hydrodynamical description, such as a change in the equation of state or in the reaction mechanism. We can introduce a scale-invariant transverse momentum per nucleon, defined as:

$$\tilde{p}^x = p^x/p^{CM}_{proj}$$

and a scale-invariant rapidity:

$$\tilde{y} = y^{CM}/y^{CM}_{proj}$$

In Fig. 1 $\tilde{p}^x$ is plotted for the experimental data obtained from Ar+KCl at 1.8 GeV/nucleon [8], La+La at 0.8 GeV/nucleon [22], Nb+Nb at 400 MeV/nucleon [11,16]. Some differences are expected, due to different multiplicity selections, different types of particles detected, and different detector bias. In spite of this, the various curves show

remarkably similar behaviours, especially for y/y_{proj} greater than -0.5. At lower rapidities the different biases of the various detectors cause a rather large spread in the values found for the transverse momenta.

Doss et al. [11] have introduced a parameter F, which they have named 'flow', defined as the slope of the transverse momentum vs. rapidity curve at mid-rapidity. This parameter, as a measure of the transverse flow, is less influenced by statistical fluctuations or detector bias than, for instance, the maximum of the curve. A scale-invariant flow, $\tilde{F}$, can be defined as [1]:

$$\tilde{F} = F/p_{proj}^{CM} \qquad (20)$$

In Fig. 2 the points for the experiments are shown, together with the $\tilde{F}$ = const. contour lines, in the A,E_{CM} plane. As was mentioned in the introduction, in [Bon 86] the behaviour of the experimental $\tilde{F}$=const. lines are compared with the curves of constant Reynolds number in the same A,E_{CM} plane. The Reynolds number characterises viscous flow patterns: Similar patterns have the same Reynolds number. For the details of the calculation of the Reynolds number see ref. [23].

The most striking difference between the Re=const. and $\tilde{F}$=const. lines appears at low energies, for $E_{CM} \leqq 60$ MeV/nucleon, indicating a drastic change either in the equation of state (e.g. a phase transition), or in the reaction mechanism. It is interesting to observe that in this energy range the Vlasov-Uehling-Uhlenbeck (VUU) model predicts a change in slope in the transverse momentum distribution [24]. Some experimental evidence for 'negative' emission angles has been found in neutron emission studies for the N+Ho reaction at 25 MeV/nucleon [25], and from measurements of the circular polarization of coincident Y-rays emitted from the residual nucleus in the N+Sm reaction at 20 and 35 MeV/nucleon [26].

This effect is due to the attractive nuclear force which, at these lower densities, overcomes the repulsive interaction due to pressure build-up. In this respect, the region of interest is at low energies.

II. STATISTICAL DESCRIPTION OF MULTIFRAGMENTATION

In the second part of the lecture we will discuss multifragmentation models and possibilities for their improvement. Multifragmentation processes play an important role in sufficiently violent nuclear collisions[27]. The many fragments in the final state of these collisions can be described in terms of statistical concepts. In particular, the specific entropy in the final state appears to be a very useful quantity. The physical reason for the usefulness of the entropy is related to the fact that the entropy/nucleon does not change significantly in the expansion stage of the collision. Entropy, therefore, provides information to the observer about the hot and dense stage of the collision.

On a more technical level, entropy is useful because it can be extracted from fragment yields with good accuracy, in contrast to quantities like the breakup temperature or density[28]. The approximate uniqueness of the entropy in the final state of central Ca + Ca and Nb + Nb collisions was demonstrated recently at beam energies in the 0.4 - 1 GeV/nucleon range [29]. Collisions at lower beam energies are also extensively studied experimentally. At these energies information on higher-mass fragments is also available [3] in addition to the yields of fragments with $A \leqq 4$. The interest in the lower energy collisions [30] is partly due to the expected liquid-vapor phase transition in nuclear matter[31]. Since the critical temperature associated with this phase transition is predicted by most models to be below 20 MeV, it is necessary to study multifragmentation at beam energies on the order of 100 MeV/nucleon.

A recent comparison of two of the most detailed static multifragmentation models (QSM and FREESCO) [32-33] showed that at high temperatures (T=30-120MeV) the two models give identical fragment distributions (Fig. 3), and furthermore they proved that the multifragmentation (represented here by the d-like to p-like ratio) [27] depends essentially on the entropy of the system. This uniform dependence on entropy only will be violated at low temperatures around T=10 MeV and below. The uniform dependence on the entropy only, was demonstrated also in an other

way too. The results of any theoretical calculation can be compared to the data utilizing a least-square procedure in terms of the theoretical (th) and experimental (exp) fragment yield ratios. Consider the quantity representing the deviation between experiment and theory:

$$\Sigma = \sum_i w_i [(Y_i/Y_p)_{th} - (Y_i/Y_p)_{exp}]^2$$

where Y_i is the yield of fragments of type i, Y_p is the proton yield and w_i is a weight factor $w_i = A_i^2/4$. In Fig. 4 we see that the model yields a minimum of this deviation at one given entropy value independent of the temperature [29]. These calculations indicate that the models are adequate to describe the observed multifragmentation satisfactorily at higher energies. Since the models are essentially based on a picture of an ideal gas mixture with a simplified repulsive interaction only (excluded volume approximation), this fit indicates that the consideration of the phase transition was not necessary.

Inclusion of interactions at the Grand Canonical level.

The majority of static multifragmentation models are based on statistical concepts [34]. The first attempt to include interactions in the statistical description of nuclear multifragmentation was made by Gross et al. [35] who included the Coulomb repulsion among the nuclear fragments in an approximate way. The two most detailed static statistical multifragmentation models FREESCO and QSM [32-33] on the other hand do not include interactions but only an excluded volume approximation, which is a simplified way of describing the hard part of the repulsive nuclear interactions.

The need for introducing attractive interactions is obvious for several reasons. The nuclear matter has a bound state, and every theoretical model which is able to describe nuclear binding leads to an EOS with a Van der Waals type first order phase transition [36]. Statistical multifragmentation models, with repulsive interactions only cannot reproduce nuclear binding,

and lead to essentially ideal gas type EOS without a phase transition. This indicates the importance of attractive interactions among nucleons and nuclear fragments at low excitation energies. While statistical multifragmentation models were very efficient in describing higher energy heavy ion collisions below a couple hundred MeV/nucleon beam energy some difficulties were observed. In deducing entropy from experimental data [2-4] light and heavy particles showed different values. Also the temperature from the population of excited states [37] did not agree with the temperature calculated from the slope of the energy spectra of emitted particles. One reason for these difficulties may be that the theoretical models used for analysing the data were neglecting attractive interactions.

Attractive interactions were included in the statistical multifragmentation models of the Copenhagen group [30]. These calculations are hard to compare with the above mentioned two statistical models (QSM [32] and FREESCO [29,33]) because instead of experimental isotope masses mass formuli are used, the breakup density and temperature were not varied systematicly so far. Thus an underlying EOS was not calculated yet either.

A part of the interactions is taken into account in the statistical models (like QSM and FREESCO) via the consideration of resonances among the possible nuclear states. This observation led Pratt et al. to the idea to include high lying resonances using the experimental information on scattering phase shifts [38]. This approach yielded an observable softening in the EOS compared to the ideal gas EOS, but it was not sufficient to result in binding and phase transition.

These observations inspired the development of new microcanonical statistical models [39,40] with the introduction of interactions among the fragments. Here we show a first preliminary attempt at the Grand Canonical level to include attractive interactions in the statistical multifragmentation model. Our further plans are to utilize this Grand Canonical statistical model later in a "FREESCO" type approximate microcanonical model where the microcanonical ensemble is generated according to this Grand Canonical expectation.

Statistical model with interactions

At the Grand Canonical level we can introduce interactions in a selfconsistent mean field approximation, similar to the way the Coulomb interactions were introduced by Gross et al. [35]. Let us consider nuclear fragments with their excited states (≈600 states with $\Gamma<1$MeV), which may move freely in a volume

$$V = A\, V_{pt} = A\, \chi\, r_0^3\, 4\pi/3 = A\, \omega_0 \qquad (21)$$

where A is the total number of nucleons, $V_{pt}=\omega_0$ is the available free volume per nucleon (which is χ times more than the available volume in ground state nuclear matter). The partition function (per one nucleon) in terms of the neutron and proton chemical potentials and temperature is $\zeta(\mu_n,\mu_p,T)$:

$$\ln \zeta(\mu_n,\mu_p,T) = \Sigma_i\, \omega_i(\mu_n,\mu_p,T) \qquad (22)$$

where the sum runs over fragments i:(A_i, N_i, Z_i)

$$\omega_i(\mu_n,\mu_p,T) = \left\{\frac{m_i\, T}{2\pi\, \hbar^2}\right\}^{3/2} V_{pt}\, \xi(i)\, e^{-(B_i+C_i+Y_i-\mu_n N_i-\mu_p Z_i)/T}. \qquad (23)$$

Here m_i is the fragment mass, B_i is its binding energy, C_i is its average selfconsistent Coulomb interaction energy with the other fragments, Y_i is its nuclear interaction with the other fragments, and $\xi(i)$ is its internal partition function.

The chemical potentials and temperature are evaluated by solving the following equations:

$$\begin{aligned} 1 &= \Sigma_i\, A_i\, \omega_i \quad , \\ Z/A &= \Sigma_i\, Z_i\, \omega \quad ,_i \\ \varepsilon &= E/A = \Sigma_i\, E_i\, \omega_i \quad , \end{aligned} \qquad (24)$$

where E is the total excitation energy of the system of A nucleons and E_i is the excitation energy of the fragment i including the kinetic energy. The abundance of a fragment of type i, in a system of A nucleons, is $A\omega_i$. The nucleons occupy a certain volume themselves the so called excluded volume: $V_{ex} = A\ 4\pi r_0^3/3$. Thus the total volume of the system consists of the volume where the fragments may move freely plus the volume occupied by the fragments: $V_{tot} = AV_{pt} + V_{ex}$. In the excluded volume approximation we consider this total volume as the physical volume of our system. The specific volume is then: $\nu = V_{tot}/A$.

If we know the selfconsistent C_i and Y_i the partition function can be evaluated. It is related to the specific free energy $\phi(T,\mu,\nu)=\varepsilon-T\sigma-\mu$ as:

$$\ln \zeta(\mu,T) = -\frac{1}{T}\,\phi(T,\mu,\nu). \qquad (25)$$

Knowing ε, T, μ, ν and $\ln\zeta$ the entropy σ and pressure p can be evaluated by:

$$\sigma = \ln\zeta - \frac{1}{T}(\varepsilon-\mu) \quad , \qquad (26)$$

$$p = -\left(\frac{\partial\varepsilon}{\partial\nu}\right)_{\sigma} \quad . \qquad (27)$$

In this way we can calculate the EOS, of our fragmentation model: $p=p(\mu,T)$. Even without interactions ($C_i=Y_i=0$) the pressure is not exactly the ideal gas pressure ($p=nT$) because of two effects: One is the excluded volume which does not allow for a compression beyond normal nuclear density n_0, and so the pressure diverges approaching n_0 [41]. The other is that the pure kinetic pressure is $p = \Sigma_i\ n_i T \neq nT$, because the fragment densities depend on the temperature. The introduction of interactions increases further the deviation from the ideal gas behaviour.

Interactions in mean field approximation

A. Coulomb interaction. To conserve simplicity and continuity we take into account the Coulomb interaction by using the approximate scheme introduced by Gross et al. [35] :

$$C_i = e^2 \frac{Z_i (Z - Z_i)}{\langle R_i \rangle} \quad , \tag{28}$$

where the average fragment distance $\langle R_i \rangle$ was calculated selfconsistently by using the following eq.:

$$\frac{1}{\langle R_i \rangle} \approx \frac{\Sigma_k Z_k \langle n_k \rangle / R_{ik}}{\Sigma_k Z_k \langle n_k \rangle} \quad , \text{ where } R_{ik} = r_{oc} (A_i^{1/3} + A_k^{1/3}) \; . \tag{29}$$

The parameter in the reported calculation was taken to be $r_{oc} = 2.36$ fm. In ref. [35] the breakup volume was not varied and only one volume was considered: $V_{pt} = A \, 4\pi \, r_1^3/3$; where $r_1 = 1.5$fm. Now since we intend to do a series of calculations at different breakup densities we vary r_1 and r_{oc} simultaneously. In the calculation of the Coulomb interaction this is the only difference between the present approach and that of ref. [35].

B. Nuclear interaction. Before we go into the details of the introduction of nuclear interactions, let us overview the basic aim of our procedure. The nuclear fragments at the breakup are in the vicinity of each other and nuclear and Coulomb interactions are not completely negligible among them. If we neglect the momentum dependent part of the interaction, in a given situation the distance between two neighbouring fragment surfaces and the radii of the fragments are the most essential factors determining the interaction. It is a straightforward procedure to utilize the "proximity potential" [42] for the description of fragment fragment interactions. The fragment radii are given by their statistical distribution in average, and the average distance between neigbouring fragments depends on the density of the system at breakup. One approach is to keep this average distance (crack

width) fixed and then depending on the other parameters (e.g. temperature or excitation energy) [30] we get a varying breakup density. If we want to describe the thermodynamic properties of the system it is, however, more straightforward to vary the breakup volume (density) and temperature (excitation energy) and then determine the "crack width" from these thermodynamic parameters.

The crack width or the distance between neighbouring fragment surfaces "d" is a quantity which strongly fluctuates. Therefore if we use the proximity potential we should average the interaction over a range of surface distances. In a Grand Canonical approach on the other hand we introduce a mean field which depends on the mean distance among the fragments only. The effect of fluctuations should be considered at this level by folding the r dependence of the proximity potential with an r distribution $f(r;d,\Delta)$ of the fragment distances centered at the average fragment distance d and having a characteristic width Δ:

$$U_{eff}(d) = \int dr\, f(r;d,\Delta)\, U_{pr.}(r) \qquad (30)$$

This folding procedure is rather approximate at the Grand Canonical level because our information about these fluctuations is limited. The resulting effective mean field potential will follow the basic features of the proximity potential but it will be smoother. For the present as a first approximate step, we introduce U_{eff} directly, instead of introducing an unknown folding distribution. In the first preliminary calculation the following simple parametrization was used, resembling the structure of the proximity potential:

$$U^{ik}_{eff}(d) = u(d)\, R_i R_k/(R_i+R_k) = V_o\, (1-a/d)\, e^{-d/b}\, R_i R_k/(R_i+R_k) \qquad (31)$$

where V_o=-160 MeV, a=1.2 fm, b=1.35 Fm. The u(d) part of the potential is plotted in Fig. 5.

We also take into account both the repulsive and the attractive part of the nuclear interaction. To do this we have to modify somewhat the "excluded volume approximation" ie. we have to allow fragments to get close to each

other to feel the repulsive hard core of the interaction. Therefore we assume that the volume of a fragment i is :

$$V_i = 4\pi/3 \; R_i^3, \text{ where } R_i = r_h + r_o(A^{1/3} - 1) \qquad (32)$$

Here the hard core radius is chosen to be $r_h = 0.4$ fm, and the radius parameter of ground state nuclear matter $r_o = 1.15$ fm. The surface of this fragment is then $S_i = 4\pi R_i^2$. Now the average excluded volume per nucleon is not the same as before but it depends on the particular fragment distribution:

$$V'_{ex} = A \, \Sigma_i \, \omega_i V_i \; . \qquad (33)$$

The total volume of the system is then: $V_{tot} = A \, V_{pt} + V'_{ex}$.

Now we can roughly estimate the distance d between neigbouring fragments at a given total physical volume (assuming that the fragment distribution is known). The total surface of all fragments is: $A \, \Sigma_i \omega_i S_i$, and the empty space among them is AV_{pt}. Deviding the latter by the former would yield a first estimate for the distance. Some part of the surface is, however, external and it is not facing other fragments. This surface can be estimated as $4\pi \, r_h^2 \, A^{2/3}$. Thus the average fragment distance between two neighbouring fragments is:

$$d \approx \frac{A \, V_{pt}}{A \, \Sigma_i \omega_i S_i - 4\pi r_h^2 A^{2/3}} \; . \qquad (34)$$

The number of fragments of type k that can surround an other fragment of type i can be estimated as:

$$N_{ik} \approx \frac{4\pi \, (R_i + R_k + d)^2}{\pi \, (R_k + d/2)^2} \qquad (35)$$

Of course, not all of the fragments around i are of type k, but only less, depending on the actual fragmentation. By somewhat underestimating the

number of surrounding fragments of type k we can assume that this number is $A\omega_k(N_{ik}/A)$.

Collecting all these ingredients the following nuclear interaction can be introduced in a mean field approximation:

$$Y_i = \frac{1}{2} \Sigma_k \, A\omega_k \, (N_{ik}/A) \, U_{eff}^{ik}(d), \qquad (36)$$

where the factor 1/2 is to avoid double counting of the interacting fragments.

The interaction depends on the particular fragment distribution, while the fragment distribution at given total energy and volume depends on the interaction. Therefore a self-consistent solution should be found. An iteration starting from non-interacting fragments was used to find the selfconsistent solution (similarly to ref. [35]).

Preliminary results

In Fig. 6 the self consistent temperature of the system is plotted versus the excitation energy for different average "crack widths" d. The system approaches ideal gas behaviour at high excitation energies and at large d-s. At large d the temperature is higher than in the ideal gas because of the attractive interaction. This result is similar to the one obtained by Bondorf et al. [30] earlier in a different model. At high densities the repulsive part of the interaction dominates leading to a decrease of the temperature.

In Fig. 7 the pressure calculated by using eqs.(26-27) is plotted versus the nuclear compression. The parameter is the excitation energy per nucleon (i.e. the curves are not the izotherms). The pressure curves show a clear first order phase transition. The critical temperature is around 30 MeV, it is somewhat higher than the usual value of T_c= 13-21 MeV. So this preliminary calculation demonstrated that the inclusion of the attractive

interactions may really lead to a liquid - gas type phase transition in a statistical multifragmentation model.

The details of the model are still to be worked out. The basic problems lie in estimating the mean interaction on the Grand Canonical level. The proper treatment of the fluctuations is a really involved problem and it might be necessary to include a temperature dependent folding distribution f(d), because we know that fluctuations increase as we approach the critical point.

The Grand Canonical approach is obviously unable to describe all the details of the fragmentation, but it can provide a useful tool and test for the Microcanonical models. It can even serve as an organic ingredient in FREESCO type microcanonical models, where the microcanonical ensemble is generated according to Grand Canonical Expectation.

Conclusions

We have seen two examples how the nuclear liquid-gas phase transition in the EOS may effect the observables in nuclear collisions. The non-scaling behaviour of the collective flow is an interesting new indirect effect. The problem of multifragmentation needs further experinmental and especially theoretical developments. One direction in this latter field was pointed out here, the need to improve the static fragmentation models by includibng attractive interactions.

Valuable contributions of Silvana Angius, Aldo Bonasera, George Fai, Joseph Kapusta, Lakshmidhar Satpathy and Bernd Schürmann to the works reported here are gratefully acknowledged. This work was supported by the National Science Foundation, grant No. - PHY-86-11210, by the San Diego Supercomputer Center and by the Italian Physical Society.

References

* On leave from the Central Res. Inst. for Physics, Budapest, Hungary

1 A. Bonasera and L. P. Csernai, Phys.Rev. Lett. 59, 630 (1987).

2 L.P. Csernai, Phys. Rev. Lett. 54, 639 (1985).

3 B.V. Jacak, H Stocker and G.D. Westfall, Phys. Rev. C29, 1744 (1984); B. Jacak, G.D.Westfall, C.K. Gelbke, L.H.Harwood, W.G. Lynch, D.K. Scott, H. Stöcker, M.B. Tsang and T.J.M. Symons, Phys. Rev. Lett. 51, 1846 (1983).; B.V. Jacak, G.D. Westfall, G.M. Crawley, D. Fox, C.K. Gelbke, L.H. Harwood, B.E. Hasselquist, W.G. Lynch, D.K. Scott, H. Stöcker, M.B. Tsang, G. Buchwald and T.J.M. Symons, preprint, MSUCL-581 (1986), Phys. Rev. C in press (1987).

4 L.P. Csernai, G. Fai and G.D. Westfall, MSUCL-605/1987 submitted to Phys. Rev. C

5 W. Scheid, H. Müller, W. Greiner, Phys.Rev.Lett. 32 (1974) 741.

6 G.F.Chapline, M.H.Johnson, E.Teller, M.S.Weiss, Phys.Rev. D8 (1973) 4302

7 H. Stöcker, L.P. Csernai, G. Graebner, G. Buchwald, H. Kruse, R.Y. Cusson, J.A.Maruhn and W.Greiner, Phys. Rev. C25 (1982)1873; A.A. Amsden, G.F. Bertsch, F.H. Harlow and J.R. Nix, Phys. Rev. Lett. 35 (1975) 905.

8 P. Danielewicz and G. Odyniec, Phys. Lett. 157B (1985) 146.

9 H.A. Gustafsson, H.H. Gutbrod, B. Kolb, H. Lohner, B. Ludewigt, A.M. Poskanzer, T. Renner, H. Riedesel, H.G. Ritter, A. Warwick, F. Weik and H. Wieman, Phys. Rev. Lett. 52 (1984) 1590.

10 P. Danielewicz and M. Gyulassy, Phys. Lett. 129B (1983) 283.

11 K.G.R. Doss, H.A. Gustafsson, H.H Gutbrod, K.H. Kampert, B. Kolb, H. Löhner, B. Ludewigt, A. M. Poskanzer, H.G. Ritter, H.R. Schmidt and H. Wieman, Phys. Rev. Lett. 57 (1986) 302.

12 C.Gale, G. Bertsch and S. Das Gupta, Phys. Rev. C35 (1987) 1666.; G.F. Bertsch, H. Kruse and S. Das Gupta, Phys. Rev. C29 (1984) 673.

13 J.J. Molitoris, J.B. Hoffer, H. Kruse, and H. Stöcker, Phys. Rev. Lett. 53 (1984) 899.

14 H. Stroebele et al., Phys. Rev. C27, 1349 (1983).

15 D. Keane et al., Proc. of the 2nd Conf. on the Interactions Between Particle and Nuclear Physics, Lake Louise, Alberta, Canada, May 1986.

16 H.G. Ritter,, K.G.R. Doss, H.A. Gustafsson, H.H. Gutbrod, K.H. Kampert, B. Kolb, H. Löhner, B. Ludewigt, A.M. Poskanzer, A. Warwick and H. Wieman, Nucl. Phys. A447 (1985)3c.

17 L.P. Csernai, P. Freier, J. Mevissen, H. Nguyen, and L. Waters, Phys. Rev. C34 (1986) 1270.

18 G. Fai, Wei-ming Zhang and M. Gyulassy, Phys. Rev. C36, 597 (1987).

19 L.P. Csernai,H. Stöcker, P.R. Subramanian, G. Graebner, A. Rosenhauer, G. Buchwald, J.A. Maruhn and W. Greiner, Phys. Rev. C28 (1983) 2001.

20 L.P. Csernai, G.Fai, J.Randrup, Phys. Lett. 140B (1984) 149.

21 N. Balazs, B. Schürmann, K. Dietrich and L.P. Csernai Nucl. Phys. A424 (1984) 605.

22 A. Sandoval, D. Bangert, R. Brockmann, C. Guerra, J.W. Harris, G. Odyniec, H.G Pugh, W. Rauch, R.E. Renfordt, D. Schall, L.S. Schroeder, R. Stock, H. Ströbele, K.L. Wolf, A. Dacal, M. E. Ortiz, GSI scientific report 1985, pg. 97, and Phys. Rev. Lett. 53 (1984) 763.

23 A. Bonasera, L.P. Csernai and B. Schurmann, MSUCL-601/1987 submitted to Nucl. Phys. A

24 J.J. Molitoris, D. Hahn and H. Stöcker, Nucl. Phys. A447 (1985) 13c.

25 F. Deák, A. Kiss, Z. Seres, G. Caskey, A. Galonsky, B. Remington, C.K. Gelbke, M.B. Tsang and J.J. Kolata, Nucl. Phys. in press.

26 M.B. Tsang, R.M. Ronningen, G. Bertsch, Z. Chen, C.B. Chitwood, D.J. Fields, C.K. Gelbke, W.G. Lynch, T. Nayak, J. Pochodzalla, T. Shea, W. Trautmann, Phys. Rev. Lett. 57 (1986) 559.

27 L.P. Csernai and J.I.Kapusta, Phys. Rep. 131, 223 (1986).

28 H. Stöcker, Nucl. Phys. A418, 587c (1984).

29 L.P. Csernai, J.I. Kapusta, G. Fai, D. Hahn, J. Randrup and H. Stöcker, Phys. Rev. C35, 1297 (1987).

30 J. Bondorf, R. Donangelo, I.N. Mishustin, C.J. Pethik, H. Schulz; and K. Sneppen, Nucl. Phys. A443, 321 (1985).;H.W. Barz, J. P. Bondorf, R. Donangelo, I.N. Mishustin and H. Schulz, Nucl. Phys. A448, 753 (1986).; J. Bondorf, J.N. De, G. Fai and A.O.T. Karvinen, Nucl. Phys. A430, 445 (1984).; S. Das Gupta, C. Gale, J. Gallego, H.H. Gan and R.D. Ratna Raju, Phys. Rev. C35, 556 (1987).

31 J.E. Finn, S. Aarval, A. Bujak, J. Chuang, L.J. Gutay, A.S. Hirsch, R.W. Minich, N.T. Porile, R.P. Scharenberg, B.C. Stringfellow and F. Turkot, Phys. Rev. Lett. 49, 1321 (1982).; P.J. Siemens, Nature 305, 410 (1983).

32 H Stocker et al. Nucl. Phys. A400, 63c, (1983).
D. Hahn and H. Stöcker, preprint, UFTP-183/1986.

33 G. Fai and J. Randrup, Nucl. Phys. A404, 551 (1983); G. Fai and J. Randrup, Comp. Phys. Comm. 42, 385 (1986).

34 A.Z. Mekjian, Phys. Rev. Lett. 38, 640 (1977).;J. Gosset, J.I. Kapusta and G.D. Westfall, Phys. Rev. C18, 844 (1978).; J. Randrup and S.E. Koonin, Nucl. Phys. A356, 223 (1981).

35 D.H.E. Gross, L. Satpathy, Meng Ta-chung, M. Satpathy, Z. Phys, A309, 41 (1982)

36 B. ter Haar and R. Malfliet, Phys. Rep. 149, 207 (1987).

37 C.K. Gelbke and D.H. Boal, preprint, MSUCL-584 (1986).

38 S. Pratt, Ph. Siemens and Q.H. Usmani, Phys. Lett. 189B, 1 (1987).

39 S.E. Koonin and J. Randrup, preprint, LBL-21165 (1986).

40 D.H.E. Gross, Zhang X.-z and Xu S.-y, Phys. Rev. Lett. 56, 1544 (1986); X.Z. Zhang, D.H.E. Gross, S.Y. Xu, and Y.M. Zheng, Nucl. Phys. A461, 641, 668, (1987).

41 L.P. Csernai and G. Fai, Acta Physica Hungarica, in press

42 J. Blocki et al. Ann. Phys. 105, 427 (1977).

Figure Captions

Fig. 1:

Scale invariant transverse momentum versus scale invariant rapidity for three different systems. (⊙) Ar+KCl at E_{lab}= 1.8 GeV/nucleon [8], (□) La+La at E_{lab}= 0.8 GeV/nucleon [22] and (<>) Nb+Nb at E_{lab} = 0.4 GeV/nucleon [16]. From [1].

Fig. 2:

Contour plots in the [A, E_{CM}] plane. Full lines in figure (a) correspond to constant Reynolds number. Full lines in figure (b) correspond to constant $\tilde{F}$. The dotted curve indicates the behavior of $\tilde{F}$ at low energies expected from the experimental results. The various symbols refer to experimental values. Symbols o, □, <>, ⊙, ∇, Δ, correspond to experimental $\tilde{F}$ values between 0.4, 0.325, 0.275, 0.225, 0.175, 0.125, and 0.1, respectively. From [1].

Fig. 3:

Plot of the d-like/p-like fragment ratio (see [29]) vs. entropy per nucleon. The full, dashed-dotted and dashed curves are calculated in the QSM model for temperatures T=30,90 and 10 MeV respectively. The symbols indicate the results obtained in the microcanonical fragmentation model FREESCO. From [29].

Fig. 4:

The quantity Σ as a function of the entropy per nucleon for the reaction Ca+Ca at 1050 MeV/nucleon, for temperatures ranging from 30 to 120 MeV. The different points at the same temperature correspond to different breakup densities. The comparison is restricted to light particles: p-α.

Fig. 5:

The effective interaction between fragments u(r) used in the interacting fragmentation model.

Fig. 6:

The temperature of the system T vs. the excitation energy per nucleon E in the interacting statictical model. Full lines correspond to constant fragment distance or 'crack width' d.

Fig. 7:

The pressure of the system vs. density n/n_0 for different excitation energies per nucleon.

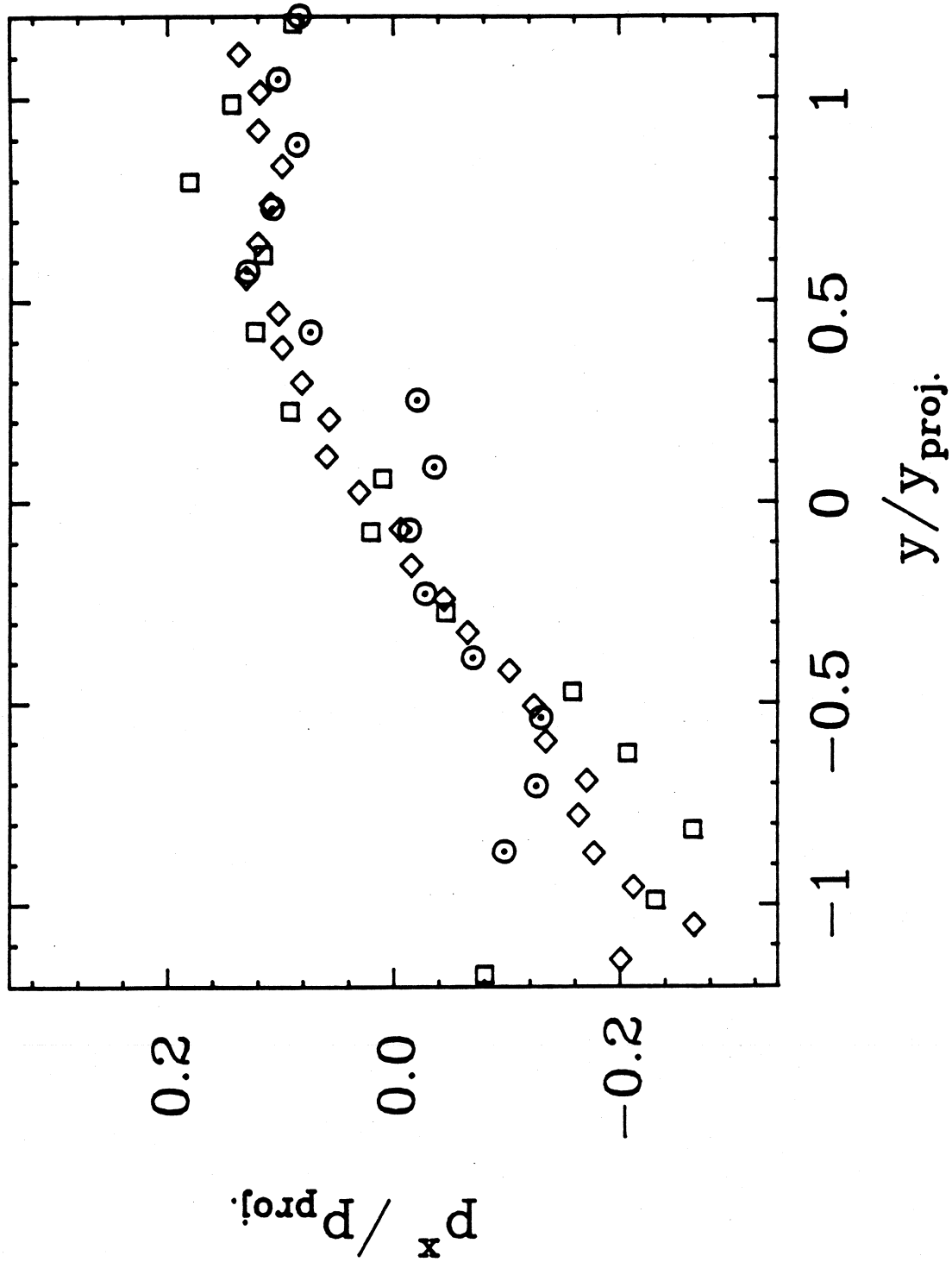

Fig. 1

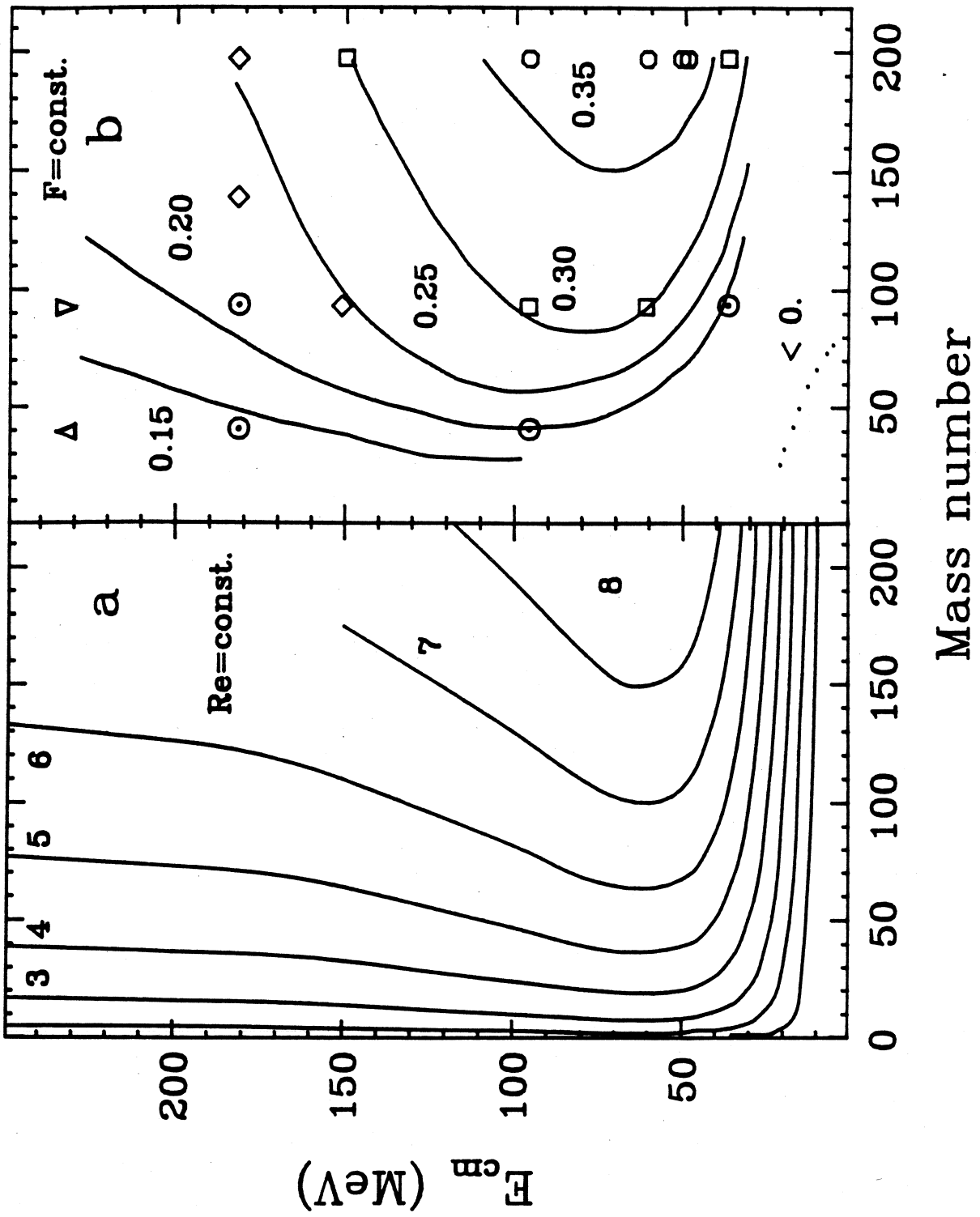
a
Re=const.
3
4
5
6
7
8
b
F=const.
0.15
0.20
0.25
0.30
0.35
< 0.
E^*_{cm} (MeV)
Mass number
0
50
100
150
200

Fig. 2

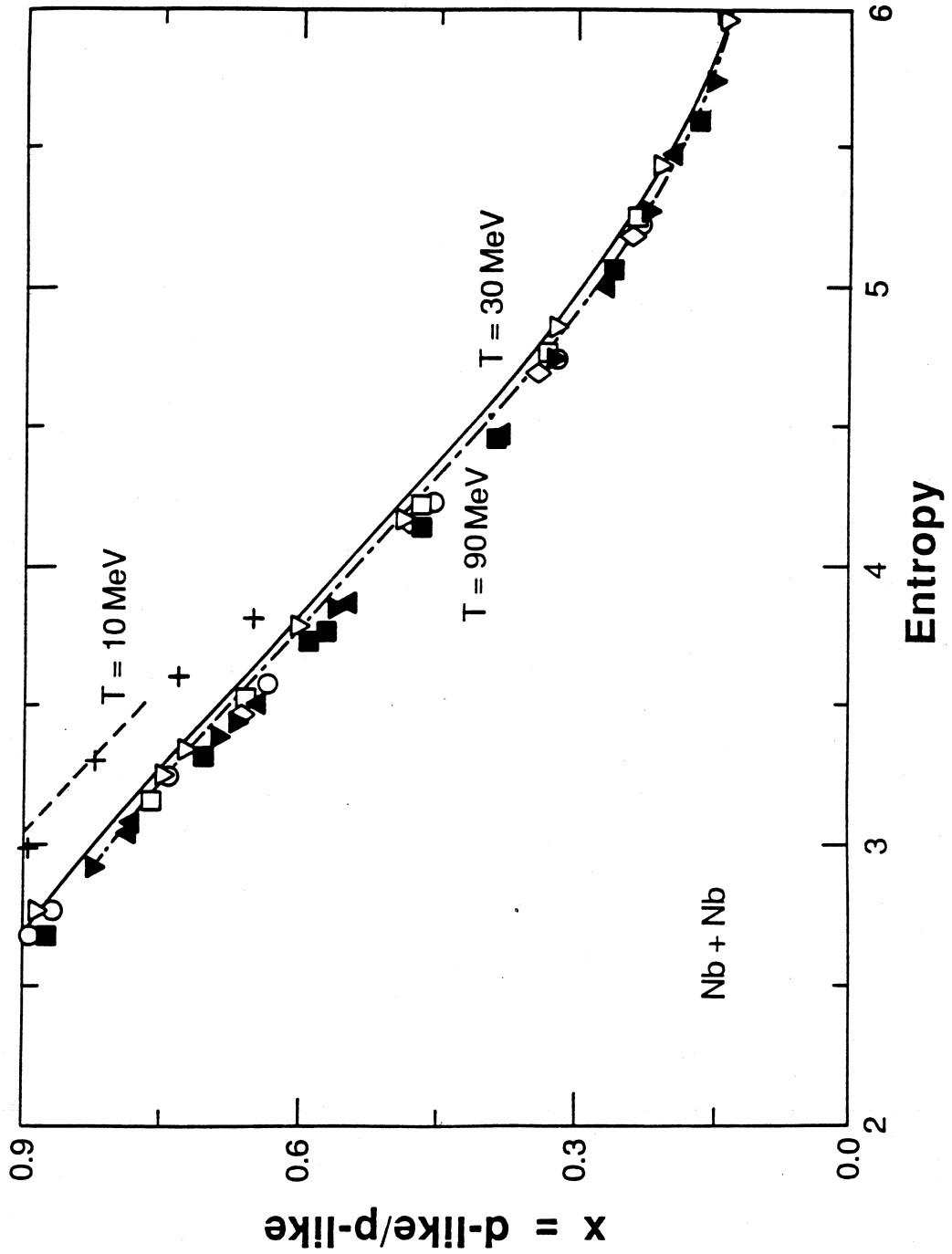
x = d-like/p-like
0.0
0.3
0.6
0.9
2
3
4
5
6
Entropy
Nb + Nb
T = 10 MeV
T = 30 MeV
T = 90 MeV

Fig. 3

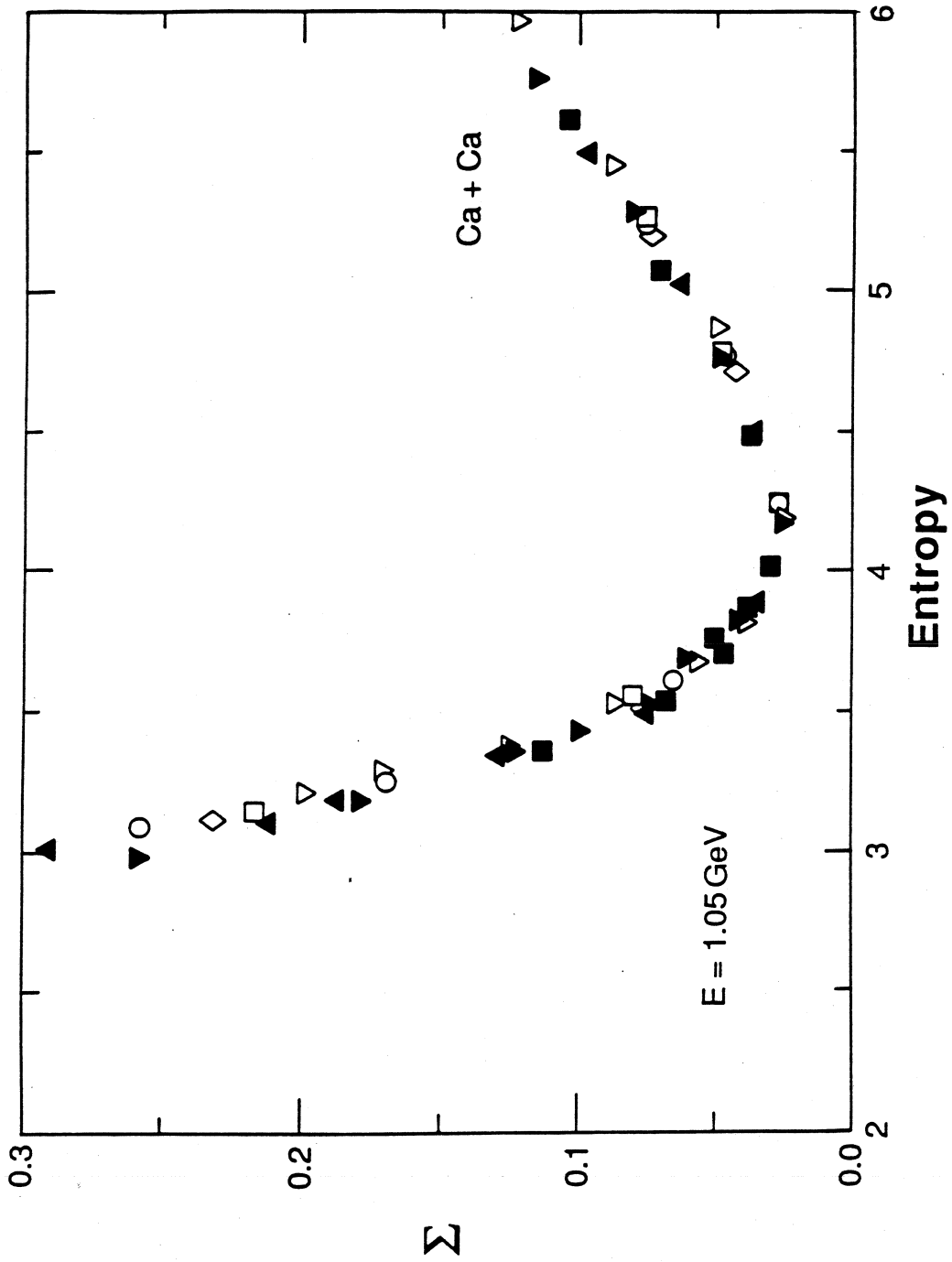

Fig. 4

MSU-87-166

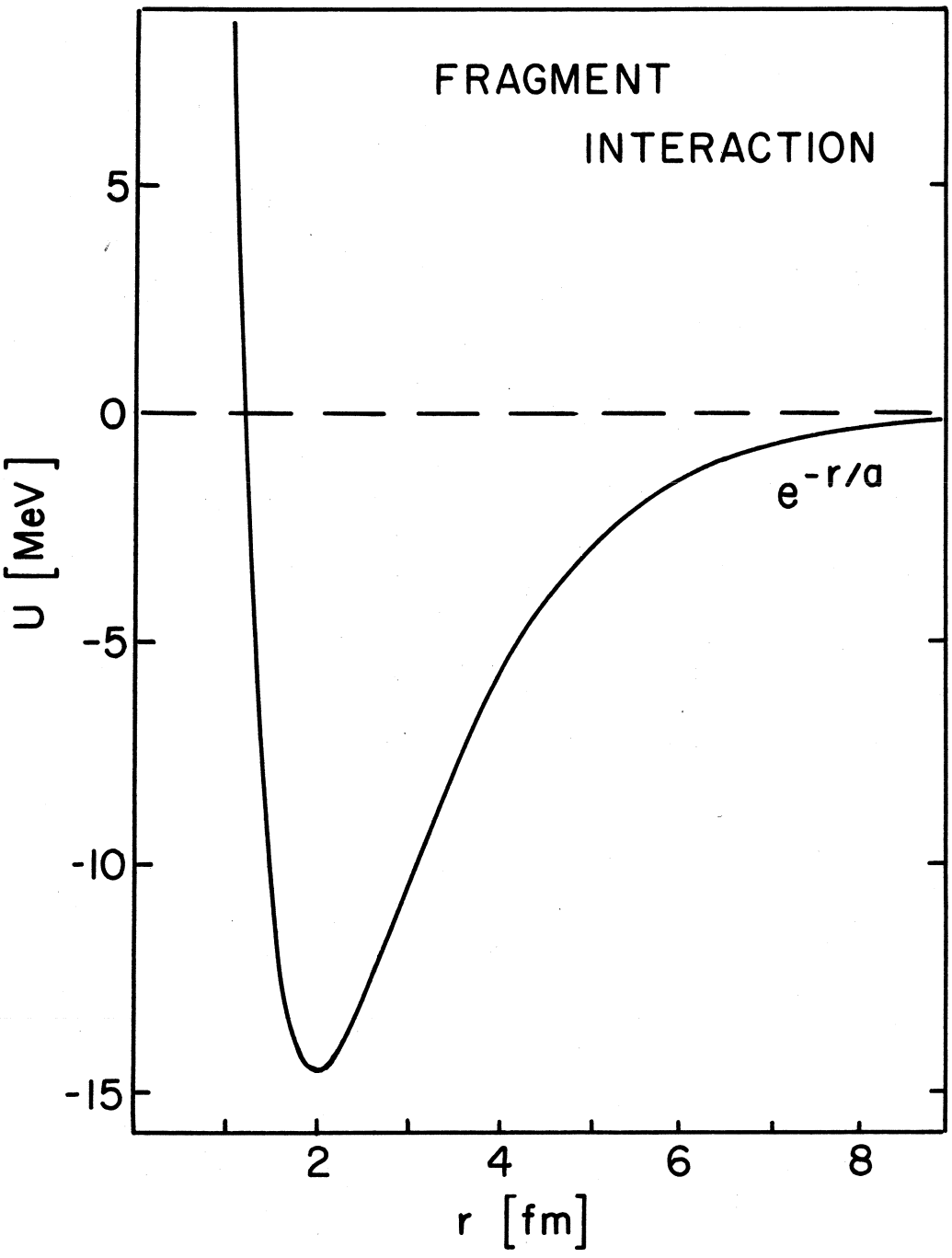

Fig. 5

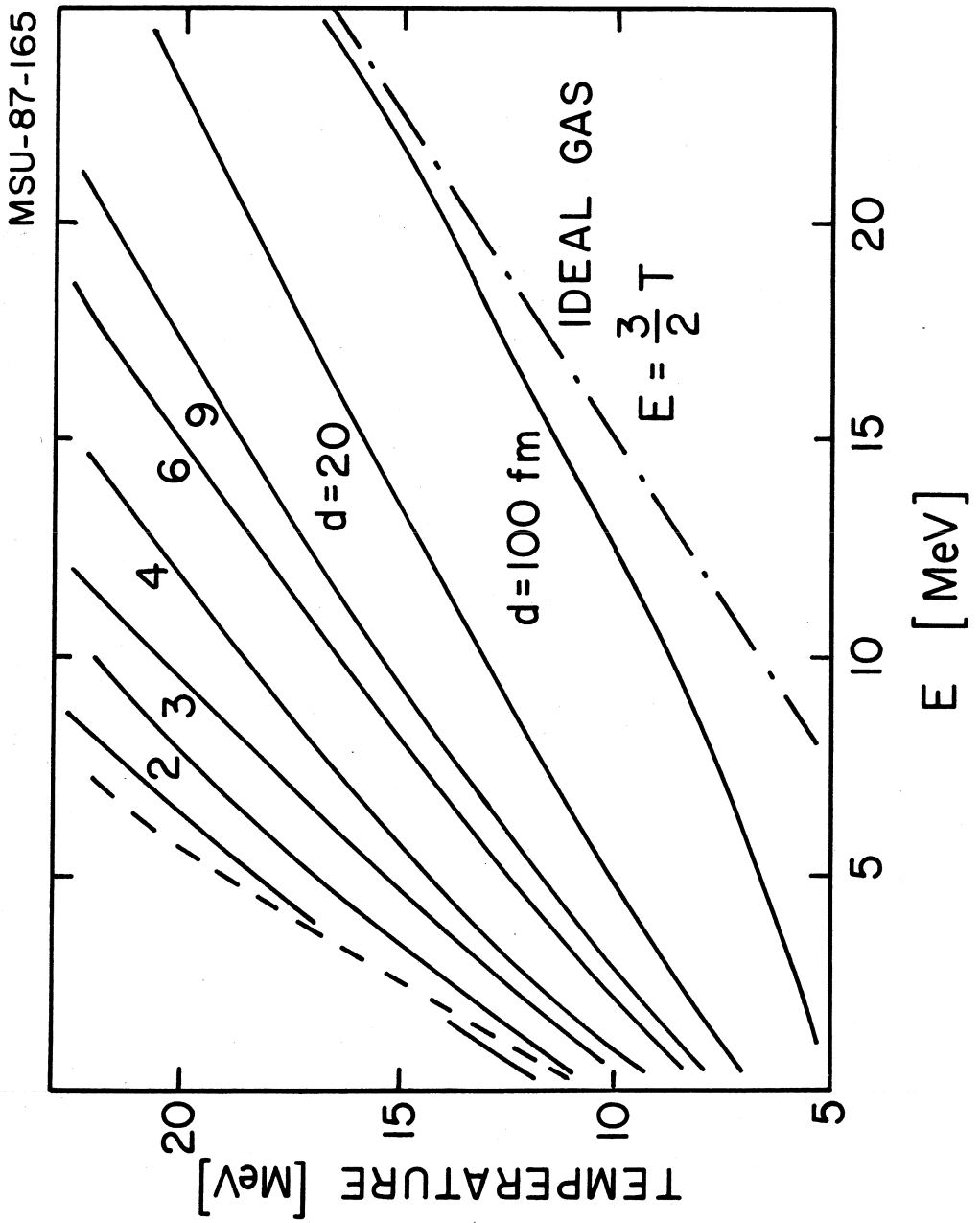
MSU-87-165
TEMPERATURE [MeV]
E [MeV]
IDEAL GAS
E = 3/2 T
d=100 fm
d=20
2
3
4
6
9
5
10
15
20

Fig. 6

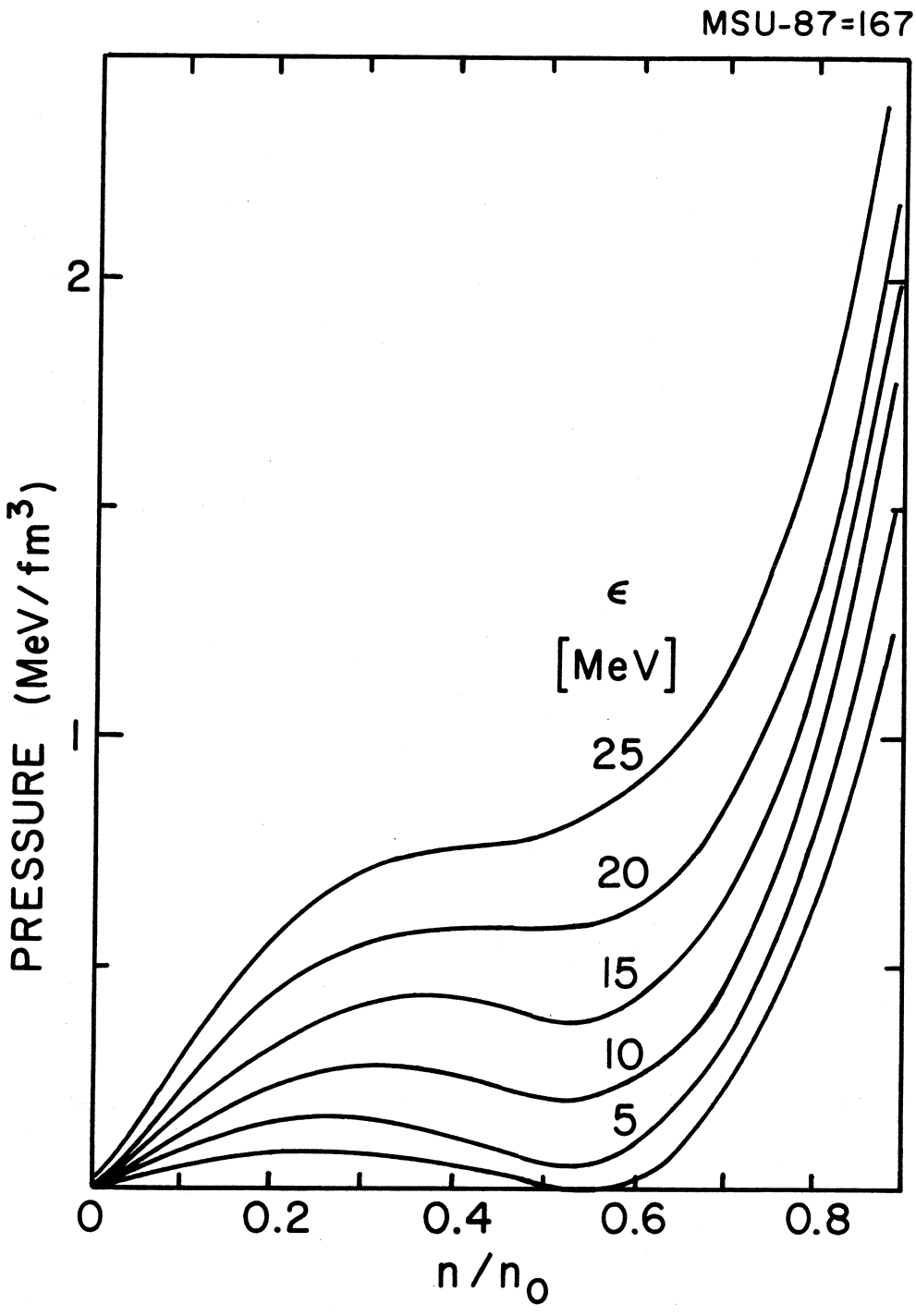

Fig. 7